Polymer Chemistry

Accepted Manuscript

ROYAL SOCIETY OF CHEMISTRY

www.rsc.org/polymers

Journal Name

RSCPublishing

ARTICLE

A multifunctional self-dissociative polyethyleneimine derivative coating polymer for enhanced gene transfection efficiency of DNA/polyethyleneimine polyplexes *in vitro* and *in vivo*

Cite this: DOI: 10.1039/xoxxoooooox

Received ooth January 2012,
Accepted ooth January 2012

DOI: 10.1039/xoxxoooooox

www.rsc.org/

Cheng Wang, Xiuli Bao, Xuefang Ding, Yang Ding, Sarra Abbad, Yazhe Wang, Min Li, Yujie Su, Wei Wang *, Jianping Zhou *

A new pH-responsive charge-conversion and rapidly self-dissociative multifunctional polymer lauric acid-polyethylenimine-cyclohexanedicarboxylic anhydride-folic acid (LA-PEI-HHPA-FA, LPHF) was developed. LPHF as an amide with neighboring carboxylic acid groups was negatively charged at physiological pH and used as a coating polymer to shield positively charged DNA/polyethylenimine 25K (DP) binary polyplexes, resulting in the formation of DPLPHF ternary polyplexes. The characterization using various methods proved that DPLPHF ternary polyplexes were stable at physiological pH, while in acidic endosomes, the coating polymer LPHF could quickly self-dissociate from the DP binary polyplexes. As compared with DP binary polyplexes, DPLPHF ternary polyplexes containing tumor targeting ligand folic acid (FA), absorption enhancer lauric acid (LA) and charge-conversion entity cis-1,2-cyclohexanedicarboxylic anhydride (HHPA) exhibited more effective cellular uptake and higher transfection efficiency with lower non-therapeutic cytotoxicity *in vitro*. Moreover, *in vivo* studies revealed significantly stronger tumor targeting and tumor inhibiting efficacy of DPLPHF ternary polyplexes. All these findings demonstrated the potential of LPHF as a promising coating polymer for enhanced gene transfection efficiency of DP binary polyplexes *in vitro* and *in vivo*.

1 Introduction

In recent years, cationic polymers such as polyethyleneimine, chitosan and poly(amidoamine) are emerging as a viable alternative to viral vectors for gene delivery, because they show significantly lower safety risks compared to viral vectors, and can also be modified to meet various needs. [1, 2, 3, 4]

Polyethyleneimine (PEI) is one of the widely studied gene delivery vectors and has already become a model polymer. There are mainly two types of PEI: linear PEI (lPEI) and branched PEI (bPEI), with different molecular weights. Among them, bPEI 25 kDa (PEI 25K) is treated as the leading polymer owing to its relatively low toxicity and high transfection efficiency. However, the remaining positive charge on the surface of DNA/PEI 25K (DP) binary polyplexes may interacts with negatively charged serum proteins (such as albumin) and red blood cells after intravenous injected into the circulatory system, hence leading to the precipitation of polyplexes in huge clusters and their adhesion to the cells surface. [5] These effects may destabilize the plasma-membrane, induce the immediate toxicity and decrease the transfection efficiency, which limited the *in vivo* application of DP binary polyplexes.

It has been reported that applying other polymers to the DP binary polyplexes surface can overcome the above-mentioned dilemma owing to the shielding of positive surface charge. [6, 7] The most extensively used method is PEGylation, [8, 9] while others considered of coating the DP binary polyplexes with some anionic polymers which have the corresponding receptor on tumor cells surface, such as hyaluronan [10] and chondroitin sulfate. [11] They both have a high affinity for CD44 receptor, thus rendering the vector "tumor targeting" ability to enhance its targeting efficiency. At the same time, the immediate toxicity is greatly reduced by changing the ternary polyplexes surface charge to a negative one with the presence of anionic polymer. However, the coverage may lower the transfection efficiency, due to the reduced cell-surface interaction, cellular uptake or endosomal escape. [12]

To improve the reduced cell-surface interaction and cellular uptake caused by anionic coating polymers, some auxiliary functional groups are required. The membrane-bound folate receptor (FR) is overexpressed on a wide range of human cancers, while

State Key Laboratory of Natural Medicines, Department of Pharmaceutics, China Pharmaceutical University, 24 Tongjiaxiang, Nanjing 210009, China
* Corresponding authors. Tel./Fax: +86 25 83271102. *E-mail addresses*: wangcpu2013@163.com (W. Wang), zhoujianpingcpu@126.com (J. Zhou).

generally absent in most normal tissues. Folic acid (FA), a small size and high affinity ligand of FR, often leads to favorable tumor-homing properties of the folate conjugates and reduced probability of immunogenicity when compared with other targeting ligands. [13, 14, 15] Moreover, hydrophobic modification has been frequently studied as an effective way to enhance gene transfection efficiency because lipid components could significantly alter some of the physicochemical and biological properties of polymers and enhance their adsorption to cell membrane. [16, 17] For instance, the transfection efficiency of bPEI 2kDa was enhanced some 400-fold by grafting lauryl groups. [18] Similar phenomena were also observed in other researches. [19, 20] Therefore, grafting FA and lauric acid (LA) to the coating polymer may greatly increase the cell-surface interaction and cellular uptake of polyplexes.

An ideal coating polymer should also be able to rapidly dissociate in a pH-responsive manner from the cationic polyplexes in the endosomes to get rid of the endosomal escape defect. Currently, many encouraging results have demonstrated that amides with neighboring carboxylic acid groups exhibit pH-dependent hydrolysis, which can lead to a negative to positive charge-reverse process on the polymer surface. [21, 22] Research indicated that PEI amidated with cis-1,2-cyclohexanedicarboxylic anhydride (HHPA) could maintain stable and negatively charged at pH 7.4 for a long time, while in acidic environments, it could readily change back to positively charged within hours, [23] which might be capable of automatically dissociating from the cationic polyplexes due to charge repulsion. [24, 25]

Enlightened by the above studies, we developed a pH-responsive and self-dissociative multifunctional coating polymer lauric acid-polyethylenimine-cyclohexanedicarboxylic anhydride-folic acid (LA-PEI-HHPA-FA, LPHF), consisting of PEI backbone, tumor targeting ligand FA, absorption enhancer LA and charge-conversion entity HHPA. Under physiological conditions, the negatively charged LPHF polymer could coat DP binary polyplexes to formulate DPLPHF ternary polyplexes, maintain their stability and circumvent the immediate toxicity in circulatory system. On the other hand, modification of PEI with FA and LA endued the polymer LPHF effective tumor targeting and uptake facilitating property, thereby enhancing the accumulation of the DPLPHF ternary polyplexes at the tumor site and promoting their cellular uptake. Lastly, in acidic endosomes, the coating polymer could become positively charged and automatically dissociate from the DP binary polyplexes due to charge repulsion. Both the exposed cationic DP binary polyplexes and the coating polymer could exert their "proton sponge" effect, facilitating DNA escape from the endosomes (Scheme 1). In this study, the proposed coating polymer LPHF was synthesized and characterized. Subsequently, the buffering capacity of polymers, and preparation optimization, stability, protection manner, particle size, zeta potential and morphology of different ternary polyplexes were analyzed. In comparison to DP binary polyplexes, *in vitro* cytotoxicity, cellular uptake and transfection efficiency as well as the intracellular trafficking of DPLPHF ternary polyplexes were all systematically investigated. Moreover, the tumor-targeting and antitumor efficacy of DPLPHF ternary polyplexes in Hela tumor xenograft nude mouse model were explored to further demonstrate their potential *in vivo* application in tumor therapy.

2. Materials and methods

2.1. Materials

1-ethyl-3-(3-dimethylaminopropyl) carbodiimide (EDC, 99%), N-hydroxysuccinimide (NHS, 98%), polyethyleneimine (PEI, branched, Mw 1.8 KDa and 25 KDa), lauric acid (LA, 99%), folic acid (FA, 98%), cis-1,2-cyclohexanedicarboxylic anhydride (HHPA, 99%), succinic anhydride (Suc, 99%) were purchased from Aladdin Reagent Inc. (Shanghai, China). The fluorescent dye FITC and Cy7 SE were obtained from Beijing Fanbo Science and Technology Co., Ltd. (Beijing, China). Hoechst 33342 and Lyso Tracker Red were offered by Invitrogen Co. (Carlsbad, CA, USA). Fetal bovine serum (FBS) and penicillin-streptomycin were obtained from Gibco (USA). Endo-free Plasmid Maxi kit was purchased from Omega Bio-Tek (USA). Bovine serum albumin, folate-deficient DMEM and 3-(4,5-dimethylthiazol-2-yl)-2,5-diphenyl tetrazolium bromide (MTT) were obtained from Sigma-Aldrich (St. Louis, MO, USA). All other chemicals and reagents otherwise stated were from Nanjing Chemical reagent Co., LTD and analytical grade.

2.2. Plasmids

Therapeutic plasmid pCMV-Neo-Bam-p53wt (p53, 8.4 kb) and reporter plasmid pEGFP-C3-hYAP1 (pEGFP-C3, 4.7 kb) used in this study were amplified in competent DH-5α *Escherichia coli* grown in LB medium containing 50 μg/ml kanamycin. Plasmids were collected and purified using an Endo-free Plasmid Maxi Kit according to the manufacturer's protocol. The quantity and quality of the purified plasmids were assessed by measuring their optical density at 260 nm and 280 nm.

2.3. Synthesis and characterization of polymers

Synthesis of LA-PEI (A): LA (23.93 mg, 0.12 mmol), EDC (68.69 mg, 0.36 mmol) and NHS (41.21 mg, 0.36 mmol) were charged into a 10 ml tube, dissolved in 5 ml of dimethyl sulfoxide (DMSO) and kept at room temperature for 30 min to activate the carboxyl groups of LA. PEI 1.8 KDa (PEI 1.8K, 107.50 mg, 0.06 mmol) was dissolved in 10 ml of DMSO in a 25 ml flask. The activated LA solution was then drop-wise added into the PEI solution with magnetic stirring. The reaction was allowed to continue with the protection of argon at room temperature for 24 h. The mixture was purified by repeated precipitation in diethyl ether. The raw product was further purified by dialysis in deionized water (MWCO 1000 Da, 2 L × 3) to remove the unreacted LA, EDC and NHS. The resulting solution was lyophilized to obtain LA-PEI.

Synthesis of LA-PEI-FA (B): FA (26.36 mg, 0.06 mmol), EDC (68.69 mg, 0.36 mmol) and NHS (41.21 mg, 0.36 mmol) were charged into a 10 ml tube and dissolved in 5 ml of DMSO. Subsequently, the reaction solution was allowed to stay in the dark for 1 h to activate the carboxyl groups of FA. LA-PEI (131.43 mg, 0.06 mmol) was dissolved in 10 ml of DMSO in a 25 ml flask. The activated FA solution was then drop-wise added into the LA-PEI solution with magnetic stirring. The reaction was performed with the protection of argon at room temperature in the dark for 24 h, after which excess diethyl ether was added to the yellowish transparent solution to induce precipitation. The raw product was further purified by dialysis in deionized water (MWCO 1000 Da, 2 L × 3) to remove the unreacted FA, EDC and NHS, prior to being freeze-dried to produce LA-PEI-FA.

Synthesis of LA-PEI-HHPA-FA (C): LA-PEI-FA (152.52 mg, 0.06 mmol) was dissolved in 10 ml of DMSO in a 25 ml flask with gentle agitation, followed by the addition of 1,2-cis-cyclohexanedicarboxylic anhydride (HHPA, 185.29 mg, 1.20 mmol). The reaction was kept at room temperature with the protection of argon in the dark for 48 h. The mixture was isolated and purified by repeated precipitation in diethyl ether, followed by desiccation under high vacuum at 40 °C for 8 h and LA-PEI-HHPA-FA (LPHF) was obtained.

Additionally, we prepared LA-PEI-HHPA (LPH), FA-PEI-HHPA (FPH) and LA-PEI-succinic anhydride (Suc)-FA (LPSF) with the same method as controls. The chemical structures of LPHF, LPH, FPH and LPSF were characterized by ^{1}H NMR (Avance™ 300, Bruker, Germany). The degree of FA grafted to PEI 1.8K was determined d by measuring the absorption value of LPHF at 286 nm with spectrophotometer (Hitachi, Japan), the grafting level of LA, HHPA, and the remaining free amino group (%) were calculated based on the grafting rate of FA and the ^{1}H NMR spectrum of LPHF.

Moreover, the buffering capacity of PEI 1.8K, LPH, FPH, LPSF, LPHF and PEI 25K from pH 7.4 to 5.1 was determined by acid-base titration. Briefly, 6 mg PEI 1.8K, 6 mg PEI 25K, 15.6 mg LPH, 16.2 mg FPH, 13.8 mg LPSF or 16.4 mg LPHF (all coating polymers were calculated to contain 6 mg PEI 1.8K equally) was dissolved in 30 ml 0.1 M NaCl and the solution was adjusted to pH 10 with 1 M NaOH or HCl. Following that, the solution was titrated with 0.1 M HCl stepwise in increments of 10 μl and the change in pH value was recorded to obtain the titration profile. The buffering capacity was calculated as the percentage of amine groups being protonated when the pH dropped from pH 7.4 to 5.1. [26]

2.4. Preparation and characterization of polyplexes

2.4.1. Preparation of polyplexes

P53 was dissolved in HEPES buffer (HEPES 20 mM, pH 7.4) to obtain a final concentration of 0.2 mg/ml, and then drop-wise added into 0.2 mg/ml PEI 25K HEPES buffer solution at the weight/weight (w/w) ratio of 1 with vortex to formulate DP binary polyplexes.

Keeping the amount of PEI 25K constant, the DP binary polyplexes solution was then drop-wise added into LPHF solution at various w/w ratios of LPHF to PEI 25K (LPHF/PEI 25K, 1 to 80) to construct a series of DPLPHF ternary polyplexes. All polyplexes used in the following study, including DPLPH, DPFPH and DPLPSF ternary polyolexes, were prepared in the same manner containing p53 unless otherwise stated.

2.4.2. Particle size and zeta potential measurements

DP binary polyplexes at the w/w ratio of 1 and a series of ternary polyplexes at different w/w ratios of coating/PEI 25K ranging from 1 to 80 were prepared at a final DNA concentration of 0.05 mg/ml. The particle size and zeta potential of polyplexes in HEPES buffer (pH 7.4) were measured by a Dynamic Light Scattering Analyzer (Brookhaven, USA) and a ZetaPlus Zeta Potential Analyzer (Brookhaven, USA), respectively.

2.4.3. Gel electrophoresis assay

The competitive dissociation potential of DNA was evaluated by agarose gel electrophoresis. Ternary polyplexes (coating/PEI 25K = 1-80, w/w) containing 1 μg p53 were loaded onto a 1 % agarose gel. At the same time, naked p53 and DP binary polyplexes were used as controls. The samples were run on the gel in 0.5 × TBE buffer at 90 V for 60 min and photographed using a Gel-Pro analyzer (Genegenius, Syngene, UK).

2.4.4. Serum stability study

The protection effect of ternary polyplexes on DNA against the degradation of DNase in the serum was determined. Polyplexes (coating/PEI 25K = 1-20, w/w) containing 200 ng DNA were incubated with 25% fetal bovine serum (FBS) for 24 h at 37 °C. The DNase in serum was then inactivated with 0.5 M EDTA (0.5-1 μl per 10 μl of serum). After the inactivation, samples were incubated with excess of heparin for 1 h to ensure complete release of DNA from the polyplexes, followed by agarose gel electrophoresis assay. Naked p53 with and without serum treatment were used as negative and positive control, respectively.

2.4.5. Bovine serum albumin (BSA) challenging

DP binary polyplexes and different ternary polyplexes were prepared and then incubated with BSA solution (pH 7.4) at the final BSA concentrations of 0.2, 0.4, 0.6 and 0.8 mg/ml for 1 h at 37 °C. The amount of DNA in each sample was fixed at 50 μg. The alteration in turbidity at 350 nm was monitored with spectrophotometer. [27] On the other hand, the change in particle size was also recorded.

2.4.6. Transmission electron microscopy

The morphological observation of different ternary polyplexes was performed by transmission electron microscopy (TEM). A drop of polyplexes solution was deposited on a lacy carbon-coated cupper grid. The excess solution was removed by a piece of filter paper. The sample was air dried and observed under a transmission electron microscope system (Hitachi, Japan) at an accelerating voltage of 80 kV.

2.4.7. The pH dependent charge-conversion and self-dissociation measurement

Ternary polyplexes were dispersed in 20 mM HEPES buffer (pH 7.4) or 20 mM acetate buffer (pH 6.0 and 5.0) and incubated in 37 °C water bath. The particle size and zeta potential of polyplexes were recorded at predetermined time intervals for 12 h. The ternary polyplexes incubated in 37 °C under different pH for 1h was centrifuged (20000 rpm, 30 min, 4 °C) using a High-Speed Refrigerated Centrifuge (CR21G, Hitachi, Japan). The supernatant was carefully and quickly collected and analyzed by spectrophotometer at 286 nm. The treated and untreated polyplexes under pH 7.4 were taken as controls.

2.5. Cell lines, cell viability assays, and in vitro characteristics of polyplexes

2.5.1. Cell culture

Human cervical carcinoma cell line (Hela) and human lung carcinoma cell line (A549) were purchased from the Cell Bank of Shanghai Institute of Biochemistry and Cell Biology, Chinese Academy of Sciences (Shanghai, China) and cultured in folate-deficient DMEM supplemented with 10% FBS, 100 U/ml penicillin and 100 μg/ml streptomycin in a humidified atmosphere of 95% air/5% CO_2 incubator at 37 °C. All experiments were performed on cells in the logarithmic phase of growth.

2.5.2. In vitro cell viability assays

The cell viability of polymers and polyplexes was assessed using the MTT assay. For cell viability assay of polymers, Hela and A549 cells were seeded at 1.0×10^4 cells/well in 96-well plates and then cultured overnight for 70-80% cell confluence. The primary growth medium was removed and replaced with 200 μl of serum-free folate-deficient medium, to which PEI 25K, LPH, FPH, LPSF or LPHF was added to achieve final concentrations of 2, 5, 10, 20, 50 and 100 μg/ml. The plates were returned to the incubator for another 24 h incubating. After that, 20 μl of 5 mg/ml MTT solution in PBS was added to each well for additional 4 h incubation. The medium was carefully removed and replaced by 150 μl of DMSO to dissolve the formazan crystals. The absorbance was measured at 570 nm using Microplate Reader (EL800, BIO-TEK Instruments Inc., USA) and untreated cells were taken as a control with 100% viability. The cell viability (%) was calculated according to the following equation:

$$\text{Cell viability (\%)} = (A_{sample}/A_{control}) \times 100\%$$

For cell viability assay of DP binary polyplexes and different ternary polyplexes containing non-therapeutic pEGFP-C3, Hela and A549 cells were seeded in 96-well plates overnight for 70-80% cell confluence and then treated with polyplexes as mentioned in above paragraph, except the concentrations of PEI 25K in samples were 2, 4, 6 and 10 μg/ml. Furthermore, we assayed the cell viability of Hela and A549 cells treated with therapeutic p53-contained DP, DPLPH, DPFPH, DPLPSF and DPLPHF polyplexes, according to the above-mentioned procedure with slight modification. In the experiment, the concentration of p53 in samples was fixed at 2 μg/ml and the treatment time was prolonged to 72 h.

2.5.3. Cellular uptake and transfection study of polyplexes containing reporter gene pEGFP-C3

For cellular uptake study, PEI 25K was labeled with FITC as previously described. [28] The FITC-labeled PEI 25K, together with reporter gene pEGFP-C3, were used to construct polyplexes. On the other hand, Hela and A549 cells were seeded into 6-well plates (1×10^5 cells/well) 24 h prior to the uptake study and incubated to reach 80% cell confluence. The freshly prepared DP, DPLPH, DPFPH, DPLPSF and DPLPHF polyplexes were added to folate-deficient culture medium (without serum or with 10% serum) at a DNA concentration of 2 μg/ml. After incubation at 37 °C for 4 h, cells were rinsed three times with PBS (pH 7.4) to thoroughly remove polyplexes that were not internalized by cells. To further determine the competitive inhibition of free folic acid, Hela cells (without serum or with 10% serum) were pretreated with 1 mM folic acid medium before the addition of polyplexes. The fluorescence intensity of cells was quantitatively analyzed by flow cytometry (Becton Dickinson, USA).

Transfection of DP, DPLPH, DPFPH, DPLPSF and DPLPHF polyplexes mediated reporter gene pEGFP-C3 in Hela and A549 cells was investigated with an additional 48 h of incubation in fresh folate-deficient medium (10% serum) after 4 h of uptake in serum-free folate-deficient medium. The expression of green fluorescent protein (GFP) in cells was observed under the inverted fluorescent microscope (OlympusIX51, Japan) and the transfection efficiency of polyplexes was quantified by flow cytometry.

2.5.4. Intracellular trafficking

Hela cells were seeded at a density of 3×10^5 cells per dish in 35 mm confocal dishes (Φ = 15 mm) and cultured in folate-deficient medium overnight. The medium was replaced with 2 ml serum-free folate-deficient medium and cells were then treated with FITC-labeled PEI 25K constructed DP and DPLPHF polyplexes containing 300 ng DNA. At different time points, cells were treated with 50 nM Lyso-Tracker Red for 30 min and rinsed three times with PBS before staining with Hoechst 33342 (10 μg/ml). The intracellular trafficking of polyplexes was observed using confocal laser scanning microscopy (CLSM, Leica TCS SP5, Germany)

2.6. In vivo tumor targeting and tumor growth inhibition study

2.6.1. In vivo imaging of tumor targeting ability

Female BALB/c nude mice (20-22 g) at 6 weeks of age were purchased from Shanghai Laboratory Animal Center (SLAC, China). All mice were housed in the SPF Ⅱ lab and given free access to folate-deficient diet and water. All procedures were conducted in compliance with our institutional and NIH guidelines for care and use of research animals. The tumor-bearing mice were produced by inoculating a suspension of Hela cells (2×10^6 cells in 0.2 ml physiological saline) subcutaneously into the left flank. When the tumor volume reached 80-100 mm^3, these mice were administered intravenously with Cy7-labeled DP, DPLPH, DPFPH, DPLPSF and DPLPHF polyplexes at a dose of 1 μg Cy7 per mouse. The *in vivo* tumor targeting efficacy and biodistribution of Cy7 labeled polyplexes were evaluated 12 h post-injection using *In Vivo* Imaging System (FXPRO, Kodak, USA) equipped with Cy7 filter sets (excitation/emission, 720/790 nm). After living imaging, the mice were sacrificed, and the tumor tissues as well as major organs (heart, liver, spleen, lung and kidney) were excised for *ex vivo* imaging using the same imaging system.

2.6.2. In vivo tumor growth inhibition

Hela tumor-bearing mice with tumor volume around 100 mm^3 were used to assay the therapeutic efficacy of DP binary polyplexes and different ternary polyplexes. The mice were divided into six groups (n = 6 per group) and treated with saline solution (the control group), DP, DPLPH, DPFPH, DPLPSF and DPLPHF polyplexes, at a dose of 20 μg p53 per mouse. Each sample was intravenously injected via tail vein every 2 days. The measurement of tumor size and mice

body weight was repeated once every 2 days before injection over a 14-day therapeutic period and the tumor volume was calculated by the formula: $(W^2 \times L)/2$, where W and L are the shortest and longest diameter, respectively.

2.7. Statistical analysis

Results are given as Mean ± S.D. Statistical significance was tested by two-tailed Student's t-test or one-way ANOVA using the software of Origin 8.0. Statistical significance was set at $^{*}P < 0.05$, and extreme significance was set at $^{**}P < 0.01$.

3. Results and discussion

3.1. Synthesis and characterization of polymers

A pH-responsive and self-dissociative multifunctional polymer LPHF, composed of PEI backbone, tumor targeting ligand FA, absorption enhancer LA and charge-conversion entity HHPA was synthesized as a coating polymer for gene delivery. Firstly, LA-PEI-FA was synthesized by conjugation of LA and FA to the PEI backbone respectively (Fig. 1A and B). The carboxyl groups of LA and FA were activated with EDC and NHS and then reacted with primary amine groups of PEI to form amide bond, resulting in the attachment of LA and FA to PEI backbone. Subsequently, the LPHF was prepared by amidation reaction between LA-PEI-FA and HHPA (Fig. 1C). Meanwhile, the polymer LPH which was short of targeting ligand FA, FPH which lacked in uptake enhancer LA and LPSF which did not possess the charge-conversion ability, [24] were prepared with the same method as controls. The ^{1}H NMR spectrum figures of LA-PEI, LA-PEI-FA and LPHF in D_2O were shown in Fig. 1D and the spectrum data of synthesized polymers were described as follows:

For LPHF, the signals appeared at δ = 8.54, 7.59, 6.68 ppm (FA), δ = 2.5-3.4 ppm (PEI), δ = 1.91, 1.84, 1.52, 1.51 ppm (HHPA), δ = 1.38, 1.15, 0.78 ppm (LA). For LPH, δ = 2.5-3.4 ppm (PEI), δ = 1.93, 1.86, 1.54, 1.51 ppm (HHPA), δ = 1.36, 1.13, 0.75 ppm (LA). For FPH, δ = 8.49, 7.54, 6.62 ppm (FA), δ = 2.5-3.4 ppm (PEI), δ = 1.92, 1.85, 1.53, 1.51 ppm (HHPA). For LPSF, δ = 8.52, 7.58, 6.68 ppm (FA), δ = 2.5-3.4 ppm (PEI), δ = 2.45, 2.34 ppm (Suc), δ = 1.38, 1.16, 0.79 ppm (LA). The grafting level of LA, FA and HHPA groups was expressed as % amino groups conjugated with LA, FA, HHPA, and the remaining free amino group % in Table 1.

It has been widely acknowledged that the high buffering capacity of polymeric gene delivery vectors, which can mediate effective release of polyplexes from endosoms via the proton-sponge effect, plays an important role in successful gene transfection. [29] In this study, coating polymer on the surface of DP binary polyplexes might be an obstacle for the escape of DP binary polyplexes from endosomes by strong proton-sponge effect of PEI 25K, so rapid dissociation of coating polymer from DP binary polyplexes was vital and this process required sufficient buffering capacity of the coating polymer. [25] Therefore, the buffering capacity of coating polymers was investigated by acid-base titration. As shown in Fig. 2, PEI 25K presented the highest buffering capacity of ~ 36% over the pH range of 7.4-5.1, while LPSF displayed the lowest one of merely ~ 7%. As expected, LPH and FPH showed similar buffering capacity to LPHF (~ 20%), only slightly impaired when compared with PEI 1.8K (~ 22%), which was sufficient for their self-dissociation from DP binary polyplexes. Moreover, after self-dissociating from the DP binary polyplexes, their buffering capacity could also exert the proton-sponge effect on favoring the endosomal release of DP binary polyplexes. Collectively, it was inferred that the buffering capacity of LPHF might promoted the endosomal escape of DP binary polyplexes and mediated high transfection activity.

3.2. Preparation and characterization of polyplexes

3.2.1. Characterization of polyplexes

A successful delivery of gene requires the vector to overcome multiple delivery barriers and the formation of stable DNA/vector polyplexes should be the primary step, so the particle size and zeta potential of DP binary polyplexes and different ternary polyplexes at different coating/PEI 25K ratio (w/w and charge ratio) were measured to verify the self-assembly of positively charged DP binary polyplexes with anionic coating polymer through electrostatic interaction. As shown in Fig. 3A, DP binary polyplexes (w/w = 1, charge ratio = 0.43) were nano-sized polyplexes (~110 nm) with highly positive surface charge (+45 mV). The addition of negatively charged LPHF to the DP binary polyplexes increased their final size up to 258.9 nm (LPHF/PEI 25K = 2, w/w, charge ratio = 0.86) and gradually decreased the zeta potential to -36.28 mV (LPHF/PEI 25K = 80, w/w, charge ratio = 34.29). In detail, the size of DPLPHF ternary polyplexes increased with the addition of coating polymer LPHF at first (LPHF/PEI 25K = 0-2, w/w, charge ratio = 0-0.86), this might due to the continuous deposition of LPHF on the surface of DP binary polyplexes. Further addition of LPHF resulted in persistent decrease of particle size until a minimum of 94.5 nm (LPHF/PEI 25K = 8, w/w, charge ratio = 3.44) and neutral zeta potential of DPLPHF ternary polyplexes was observed. Subsequent addition of LPHF slightly increased the particle size but greatly decreased the zeta potential until the LPHF/PEI 25K (w/w) ratio up to 20 (charge ratio = 8.57). When the w/w ratio of LPHF/PEI 25K was more than 20, both particle size and zeta potential remained stable, with only few changes. The results indicated that LPHF was actually deposited onto the DP binary polyplexes, leading to the formation of DPLPHF ternary polyplexes. DPLPH, DPFPH and DPLPSF ternary polyplexes showed similar changes to DPLPHF in both particle size and zeta potential measurements (Fig. S1).

Excess addition of polyanions usually leads to the decomposition of the polyplexes owing to competitive dissociation of the DNA molecule from the PEI. [30] Thus, gel electrophoresis assay was performed to determine the retardation of DNA and optimize the w/w ratio of coating to PEI 25K in different ternary polyplexes formulations. The electrophoresis result of DPLPHF ternary polyplexes was shown in Fig. 3B, we observed that no retardation was found with naked pDNA alone, while complete retardation of DNA was observed in DP binary polyplexes. For DPLPHF ternary polyplexes at w/w ratios of LPHF to PEI 25K ranging from 1 to 20, complete retardation without any leakage of DNA could also be attained. Interestingly, continuous increment of LPHF until a w/w ratio of 40 caused minor release of DNA from the polyplexes as expected, and more DNA was released from the polyplexes at the LPHF/PEI 25K ratio (w/w) of 80 as supported by brighter bands. The similar change trends in the DPLPH, DPFPH and DPLPSF ternary polyolexes groups were also presented (Fig. S2). Taking the results from polyplex-formation and DNA dissociation analyses into consideration, it was evidenced that all the ternary polyplexes at the coating to PEI 25K w/w ratio of 20 with moderate particle size and zeta potential (100 nm and -26.67 mV for

DPLPHF ternary polyplexes) were optimal and were selected as model polyplexes in the following experiments.

After effective package of DNA, polyplexes were usually intravenously injected into the circulatory system where they have to across various extracellular barriers, including interactions with blood components, degradation of therapeutic DNA by serum nucleases, and so on. [31] As a result, we performed serum stability and BSA challenging assays to further determine the well protection and stability of DNA in polyplexes. The protective effect of the polyplexes on DNA against serum nucleases degradation was assessed by the co-culture of polyplexes with serum. Naked DNA was completely degraded after incubation in 25% FBS for 24 h (Fig. 3C). In contrast, all the DPLPHF ternary polyplexes, even ones at the lowest ratio of LPHF to PEI 25K (w/w = 1) exerted strong protective effect on DNA, as supported by the comparable intensity and width of bands to the positive control (naked DNA without serum). For BSA challenging experiment, as revealed in Fig. 3D, higher BSA concentration tended to induce more significant instability of positively charged DP binary polyplexes. However, DPLPHF ternary polyplexes with reduced surface charge exhibited evident superiority in suppressing protein adsorption to DP binary polyplexes, which was expected from the results of zeta potential measurement. Compared with DP binary polyplexes, for DPLPHF ternary polyplexes with LPHF to PEI 25K w/w ratio of 1, slower increase in OD_{350nm} appeared, at w/w ratio of 5, significant decline in the variation of OD_{350nm} was observed, indicating that higher w/w ratio of LPHF to PEI 25K contributed to alleviate aggregation tendency induced by negative protein. At the w/w ratio of 10, the surface charge of DPLPHF ternary polyplexes became almost neutral and the turbidity change was almost negligible. It was worth noting that DPLPHF ternary polyplexes at the LPHF to PEI 25K w/w of 20 showed the greatest stability without any increment in OD_{350nm}. Same conclusions could also be drawn from the change results of particle size (Fig. 3D). The serum stability and BSA challenging results obtained from DPLPH, DPFPH and DPLPSF ternary polyplexes were similar to DPLPHF ternary polyplexes and they all showed strong protective effect against serum and BSA at the coating/PEI 25K ratio (w/w) of 20 (Fig. S2 and S3).

Moreover, the morphology of the optimized ternary polyplexes (coating/PEI 25K = 20, w/w) was observed using TEM and the result of DPLPHF ternary polyplexes was shown in Fig. 3F. All the polyplexes exhibited compact spherical shape with size around 100 nm. A core-shell structure was also found, implying that LPHF polymer was actually anchored on the surface of DP binary polyplexes. The morphology of DPLPH, DPFPH and DPLPSF ternary polyplexes were displayed in Fig. S4. Likewise, they were all spherical nanoparticles with core-shell structure.

3.2.2. The pH dependent charge-conversion and self-dissociation measurement

The DPLPHF ternary polyplexes were expected to remain stable in physiological conditions (pH 7.4), and self-dissociate, followed by the release of positively charged DP binary polyplexes under acidic conditions (pH 6.0 and 5.0). Thus, the particle size and zeta potential of DPLPHF polyplexes at pH 7.4, 6.0 and 5.0 were examined to investigate the pH-responsive property of LPHF as a coating polymer.

The optimized DPLPHF ternary polyplexes were prepared, dispersed in HEPES buffer (pH 7.4) or acetate buffer (pH 6.0 and 5.0) and incubated in 37 °C water bath. The particle size and zeta potential were monitored at prearranged time points for 12 h. As shown in Fig. 4A, DPLPHF ternary polyplexes remained stable under physiological condition without evident change in particle size and zeta potential. However, significant increase in particle size and zeta potential was observed at pH 6.0. In detail, large aggregates with a particle size of over 1 μm and zeta potential of +7.63 mV formed within 1 h, which was consistent with Lee's report. [24] Interestingly, at pH 5.0, the DPLPHF ternary polyplexes immediately became positively charged (+29.82 mV) and gradually reached a zeta potential of about +43.06 mV in 1 h. The particle size of polyplexes increased slightly to around 210 nm and no aggregation visualized. LPHF is an amide with neighboring carboxylic acid groups, which exhibits pH-dependent hydrolysis. There are two kinds of amides in LPHF. The amide of the secondary amine almost instantly hydrolyzed at pH 5.0, slightly slower at pH 6.0, the amide of the primary amine hydrolyzed more slowly at pH 5.0 and 6.0 than that of the secondary amine amide. [23] The different hydrolysis speed of two different amines could be responsible for the different phenomena mentioned above. At pH 6.0, the secondary amine gradually hydrolyzed to restore the positive nature of PEI 1.8K. The slow loss of negatively charged carboxyl groups and increase of positively charged amino groups might generated swelling of DPLPHF ternary polyplexes and finally led to interaction and aggregation of neighbouring polyplexes. In contrast, at pH 5.0, the secondary amine almost instantly hydrolyzed and the hydrolysis of primary amine was also accelerated. The drastic decrease of negatively charged carboxyl groups and increase of positively charged amino groups might induce strong repulsive force between LPHF and DP binary polyplexes, which triggered immediate dissociation of LPHF polymers. The dramatic dissociation process left no opportunity for the interaction and aggregation of neighbouring polyplexes.

The pH-dependent self-dissociation behaviour of LPHF was further confirmed by employing a centrifuge method. High-speed centrifuge can precipitate the polyplexes while maintaining the self-dissociated LPHF in the supernatant. The picture and calculated remaining LPHF polymers in the supernatant of different samples were displayed in Fig. 4B. The treated and untreated polyplexes at pH 7.4 were set as controls with remaining LPHF ratio of 0% and 100%, respectively. As compared with untreated polyplexes at pH 7.4, the remaining LPHF ratio of polyplexes at pH 6.0 was merely 21.71%, indicating that most of the LPHF polymers were still attached on the surface of DP binary polyplexes. In contrast, the polyplexes at pH 5.0 showed a remaining LPHF ratio of 93.26%, demonstrating that the dissociated LPHF polymers were in the majority. The DPLPH, DPFPH and DPLPSF ternary polyplexes were also tested in the same way. DPLPH and DPFPH polyplexes showed similar properties to DPLPHF ternary polyplexes while DPLPSF polyplexes remained almost the same in all three buffer solutions as expected (Fig. S5). Taken together, the above results demonstrated that coating polymer LPHF containing charge-conversion entity HHPA could remain stable under physiological conditions and rapidly self-dissociate in endosomes, which might

favor the following endosomal escape of DP binary polyplexes and achieve significant enhancement in gene transfection.

3.3. *In vitro* cell viability and characteristics of polyplexes

3.3.1. Cytotoxicity of polymers and polyplexes

Hela cells are folate receptor overexpressing cancer cell line and A549 cells are folate receptor deficient cancer cell line. [32, 33] Both cells were treated with various concentrations of PEI 25K or coating polymers ranging from 2 to 100 μg/ml to test the cytotoxicity of polymers. As presented in Fig. 5A, inhibitory effects of PEI 25K on both Hela and A549 cells were observed in a concentration-dependent manner. PEI 25K displayed 79.11% mortality on Hela cells and 89.32% mortality on A549 cells at 100 μg/ml, which might related to its considerable positive charge. In contrast, cells in all coating polymer groups yielded a similar viability to control group (untreated cells), even at the highest concentration of 100 μg/ml, suggesting that LPHF was a safe polymer with low cytotoxicity.

Polyplexes with positive surface charge usually mediate undesired toxic effects, [34, 35] however, polyplexes with hydrophobic modification or polyanion coating on the surface can exert alleviated cytotoxicity, resulting from the reduction of their positive charge. [18, 36] As a result, the cytotoxicity of DP and different ternary polyplexes containing non-therapeutic pEGFP-C3 against Hela and A549 cells was assayed to validate whether negatively charged coating polymer with reduced positive charge could decrease the *in vitro* non-therapeutic cytotoxicity of DP binary polyplexes. As shown in Fig. 5B, compared with DP binary polyplexes in all PEI 25K concentrations, the cell viability of ternary polyplexes was higher. Especially at the concentration of 10 μg/ml, the serious cytotoxicity of DP binary polyplexes was dramatically decreased after shielding, indicating that LPHF as a coating polymer could indeed lower the non-therapeutic cytotoxicity of DP binary polyplexes.

On the other hand, it was interesting to note that at the working DNA concentrations of transfection (< 2 μg/ml), all polyplexes were not significantly toxic, so the cell viability of Hela and A549 cells treated with polyplexes containing therapeutic p53 at a concentration of 2 μg/ml was performed to test the therapeutic effect of polyplexes. As shown in Fig. 5C, all polyplexes showed cytotoxicity effect to some extent. In detail, DP binary polyplexes displayed a cell viability of 74.22% on Hela cells and 68.59% on A549 cells after 72 h treatment, which should ascribed to the therapeutic effect of p53. More importantly, DPLPHF ternary polyplexes exhibited a viability of 35.52% and 44.65% on Hela and A549 cells, respectively, which was superior to DP binary polyplexes in both cell lines. All the above data suggested that LPHF could be a safe polymer with the potential to decrease the non-therapeutic cytotoxicity and enhance the therapeutic efficacy of DP binary polyplexes, and might be a promising coating polymer *in vivo*.

Apart from the above-mentioned results, some interesting phenomena were also obtained in p53 cytotoxicity assay. Firstly, compared with DP binary polyplexes in FR-positive Hela cell line, the cytotoxicity of FA containing ternary polyplexes were all significantly higher (44.35%, 68.26%, 35.52% cell viability for DPFPH, DPLPSF and DPLPHF ternary polyplexes, respectively) while they all suffered great decline in FR-negative A549 cell line (80.70%, 73.69%, 44.65% cell viability for DPFPH, DPLPSF and DPLPHF ternary polyplexes, respectively). These results raised the possibility that FA containing polyplexes were internalized via FR-mediated endocytosis. On the other hand, the mortality of DPLPH ternary polyplexes in both cell lines was higher than DP binary polyplexes (31.85% in Hela and 51.86% in A549), which could be the combined effect of LA and HHPA or anyone of them alone. Noticeably, DPLPHF ternary polyplexes containing charge-conversion entity HHPA were more deadly than DPLPSF ternary polyplexes in both cell lines (cell viability, 35.52% versus 68.26% in Hela cells and 44.65% versus 73.69% in A549 cells), which we speculated may be due to the readily endosomal escape induced by the self-dissociation property of LPHF. All the above speculation should be validated by further investigation.

3.3.2. Cellular uptake and transfection study of polyplexes containing reporter gene pEGFP-C3

A detailed investigation concerning the cellular uptake and transfection of polyplexes using reporter gene pEGFP-C3 was conducted to find out the reasons responsible for the discrepancy in p53 cytotoxicity assay. To make sure that the cellular uptake and transfection of FA containing polyplexes occurred in a folate receptor-mediated specific manner, comparative cellular uptake and transfection of all polyplexes were estimated using Hela and A549 cell lines. Fig. 6A and B represented the flow cytometric profile and fluorescence intensity of different polyplexes with or without serum in each cell line, respectively. Compared with serum-free conditions in both cell lines, the fluorescence intensity of all polyplexes in 10% serum medium decreased. DP binary polyplexes suffered an approximately 2.68- and 2.49- fold drop in Hela and A549 cells, respectively. In contrast, such a great decrease was not observed in all ternary polyplexes, which indicated the addition of coating polymer to the cationic DP binary polyplexes enhanced their serum resistance ability. Moreover, in both cell lines, DPLPH ternary polyplexes achieved almost the same level of fluorescence intensity to DP binary polyplexes in serum-free conditions, and even higher than DP binary polyplexes in the presence of serum, regardless of their negatively charged shielding which might hindered the adsorption of polyplexes to the cell surface. This could be attributed to the uptake facilitating property of LA. On the other hand, in serum free conditions, DPFPH, DPLPSF and DPLPHF ternary polyplexes in FR-positive Hela cells exhibited significantly stronger fluorescence intensity than DP binary polyplexes (1.52-, 1.99- and 2.16-fold, respectively) while in FR-negative A549 cells, their fluorescence intensity was dramatically reduced (0.32-, 1.04- and 1.20-fold, respectively). The uptake efficiency difference of FA containing polyplexes between Hela and A549 cells might be due to the difference in FR expression level in two cell lines, providing preliminary evidence that FA containing polyplexes were transported into Hela cells via FR-mediated endocytosis. To further confirm the FR-mediated uptake, an excess amount of free folate was added in the medium to examine whether it would inhibit the cellular uptake within Hela cells by competitive binding to folate receptors. As shown in Fig. 6C and D, compared with untreated groups in both serum-free and 10% serum conditions, the fluorescence intensity of DPFPH, DPLPSF and DPLPHF ternary polyplexes in Hela cell line was effectively suppressed to a lower grade with the presence of excess folate, while the fluorescence intensity of DPLPH ternary polyplexes remained unaffected, supporting the role of folate receptor-mediated targeting of FA containing coating polymers.

The following pEGFP-C3 transfection results shown in Fig. 7 revealed more interesting facts. First of all, taken the cellular uptake

and pEGFP-C3 transfection results of DP binary polyplexes and DPLPH ternary polyplexes together, we can observed that although the uptake profile of DP binary polyplexes in serum-free medium was superior to DPLPH ternary polyplexes in both cell line, however, DPLPH ternary polyplexes in serum-free medium showed 1.71- and 1.41- fold increases in transfection efficiency compared with DP binary polyplexes in Hela and A549 cells, respectively. In addition, despite their close uptake intensity in serum-free medium, the pEGFP-C3 transfection efficiency of DPLPHF ternary polyplexes was 2.67- and 2.97-fold higher than that of DPLPSF ternary polyplexes in Hela and A549 cells, respectively. These observations provided decisive evidence that the self-dissociation property of HHPA containing polymers did contribute to their higher transgene activity, possibly via the combined "proton sponge" effect of HHPA containing polymer and PEI 25K. Furthermore, it was worth mentioning that in Hela and A549 cell lines, the pEGFP-C3 transfection efficiency of DPLPHF ternary polyplexes was always the highest and was even 5.06- and 1.96-fold higher than that of DP binary polyplexes, which was consistent with the p53 cytotoxicity results. Overall, our observations revealed that tumor targeting ligand FA, absorption enhancer LA and charge-conversion entity HHPA were all contribute to the advanced cellular uptake and transfection efficiency of DPLPHF ternary polyplexes and the combination of these three entities was more powerful than applying them alone. On the other hand, our results also raised the possibility that LPHF was a selective and effective coating polymer for enhanced gene transfection efficiency of DP binary polyplexes *in vitro*.

3.3.3. Intracellular trafficking of polyplexes

To further explore the combination effect of FA, LA and HHPA, the intracellular distribution behaviour of DP and DPLPHF polyplexes was investigated. The polyplexes were constructed by FITC labeled PEI 25K (green color), the endosomes were stained with Lyso-Tracker Red (red color) and the nuclei were stained with Hoechst 33342 (blue color), so the location of polyplexes can be visualized (Fig. 8). At 0.5 h, DP binary polyplexes with slight green fluorescence was observed around Hela cells (Fig. 8A), in contrast to more fluorescent dots attached on cell surface with the treatment of DPLPHF ternary polyplexes (Fig. 8B). As expected, more obvious difference between DP binary polyplexes and DPLPHF ternary polyplexes was found at 1.5 h. DP binary polyplexes started to enter the endosomes with slight green color luminescent with red color (endosomes). However, DPLPHF ternary polyplexes exhibited more intense green fluorescence in the endosomes, implying the efficient internalization of DPLPHF ternary polyplexes via the synergistic effect of tumor targeting ligand FA and absorption enhancer LA. In particular, at 3 h, most of the DP binary polyplexes were still in the endosomes, with only a small portion of green dots appeared in the nuclei (green color merged with blue color), while it was worth mentioning that many DPLPHF ternary polyplexes were localized in the nuclei, suggesting their rapid endosomal escape, which might benefit from the self-dissociation process induced by the charge-conversion entity HHPA of LPHF. Taken together, the above results indicated that coating polymer LPHF containing three functional entities could not only increase the amount of cellular uptake but also facilitate the endosomal escape of DPLPHF ternary polyplexes, which was beneficial for the enhancement in gene transfection efficiency.

3.4. *In vivo* tumor targeting and tumor growth inhibition study

3.4.1. *In vivo* targeting efficacy

It is well known that DP binary polyplexes with strong positive charge always present poor tumor targeting efficacy *in vivo*. DP binary polyplexes applied with our coating polymer have exhibited preferable serum resistance and cellular uptake efficacy *in vitro*, so improved tumor targeting efficacy of ternary polyplexes *in vivo* can be expected. Here, the targeting behaviour of polyplexes in Hela tumor-bearing nude mice was evaluated using an NIR fluorescence imaging system. Fig. 9A showed the *in vivo* fluorescence intensity of Cy7 at the tumor site after 12 h of intravenous injection of polyplexes. There was significant difference in targeting efficacy between DP binary polyplexes and different ternary polyplexes. In detail, the fluorescence intensity of all ternary polyplexes at the tumor site was stronger than that of DP binary polyplexes, especially the FA containing ternary polyplexes. A similar conclusion can be reached by the *ex vivo* results of tumor and main organs. As shown in Fig. 9B and C, shielding with polymers led to much more accumulation of polyplexes in tumor sites, for instance, the fluorescence intensity of DPLPHF ternary polyplexes in the tumor was 6.73-fold stronger than that of DP binary polyplexes. In contrast, DP binary polyplexes showed preferable uptake by the reticuloendothelial system (RES), the accumulation of DP binary polyplexes in the liver was more than in the others, which was consistent with previous studies. [37, 38] This might in part attribute to their poor tumor targetability. Furthermore, it is noteworthy that the fluorescence intensity of both DPLPSF and DPLPHF ternary polyplexes was more intense than that of DPLPH or DPFPH ternary polyplexes, further demonstrating that stronger targetability can be achieved via the synergistic effect of tumor targeting ligand FA and absorption enhancer LA. Altogether, it can be inferred that coating polymer LPHF might be capable of changing the behaviour of the DP binary polyplexes and suitable for tumor-specific delivery of gene, based on which the strong therapeutic effect of p53 gene in tumor growth inhibition *in vivo* can be expected.

3.4.2. *In vivo* tumor growth inhibition

The *in vivo* anti-tumor effect of DP binary polyplexes and different ternary polyplexes was evaluated by measuring the tumor volume and body weight of the mice following the treatment. Fig. 10A revealed that all the polyplexes showed anti-tumor effect to some extent. However, the tumor growth inhibition efficacy in all ternary polyplexes groups was significantly higher than that in DP binary polyplexes and they followed an order: DPLPHF > DPFPH > DPLPSF > DPLPH, DPLPHF ternary polyplexes appeared to be the most potent formulation with final tumor volumes of 189.38 ± 45.71 mm^3, which was in line with p53 cytotoxicity and pEGFP-C3 transfection results, further confirming the superiority of coating polymer LPHF. In addition, the body weight variation of the tested mice was shown in Fig. 10B. The body weight of mice in saline and DP binary polyplexes groups suffered continuously decrease with the increase of treatment time, indicating that the living quality of mice was compromised. In contrast, no noticeable change in body weight was observed in all ternary polyplexes groups, suggesting their safety for *in vivo* application. In summary, our data demonstrated that multifunctional LPHF could be used as a safe and effective tumor-targeting and transfection-enhancing coating polymer for controlling the tumor growth *in vivo*.

4. Conclusions

In our study, a new multifunctional coating polymer LPHF with dual auxiliary groups (tumor targeting ligand FA and uptake facilitating entity LA) and charge-conversion property was successfully synthesized to overcome the obstacles of gene delivery, including tumor accumulation, cellular uptake and endosomal escape. LPHF could anchor on the surface of DP binary polyplexes via electrostatic interaction at physiological pH, leading to the formation of DPLPHF ternary polyplexes, and self-dissociate to assist the endosomal escape at acidic pH. The well-formed DPLPHF ternary polyplexes with improved stability against serum and BSA, exhibited significantly inhibitory effect of polyplexes containing p53 on Hela and A549 cells, mediated markedly elevated gene transfection and potentiated intracellular delivery in FR-overexpressed Hela cells *in vitro*, owing to FA and LA associated specific and effective cellular uptake, as well as their rapid self-dissociation property. Moreover, *in vivo* investigation on nude mice bearing Hela xenografts confirmed that DPLPHF ternary polyplexes exerted high tumor-targeting capacity and strong anti-tumor efficacy. Altogether, as a negatively charged coating polymer, LPHF could apply on DP binary polyplexes and might offer a very powerful approach to improve their transfection efficiency *in vitro* and *in vivo*.

Acknowledgments

We gratefully acknowledge Prof. Yunman Li and her group members for providing cell laboratory and technical support, as well as Prof. Hu-lin Jiang and his group members for offering advises and experimental apparatus. We also appreciate the financial support from the National Natural Science Foundation of China (Nos. 81102398 and 81273469) and the Natural Science Foundation of Jiangsu Province (No. BK2011624).

References

1. T. Merdan, J. Kopeček and T. Kissel, *Advanced Drug Delivery Reviews*, 2002, **54**, 715-758.
2. G. Wang, H. Yin, J. C. Y. Ng, L. Cai, J. Li, B. Z. Tang and B. Liu, *Polymer Chemistry*, 2013, **4**, 5297-5304.
3. B. Shi, H. Zhang, Z. Shen, J. Bi and S. Dai, *Polymer Chemistry*, 2013, **4**, 840-850.
4. Y. Sun, Y. Jiao, Y. Wang, D. Lu and W. Yang, *International journal of pharmaceutics*, 2014, **465**, 112-119.
5. H. Lv, S. Zhang, B. Wang, S. Cui and J. Yan, *Journal of Controlled Release*, 2006, **114**, 100-109.
6. R. Kircheis, L. Wightman, A. Schreiber, B. Robitza, V. Rössler, M. Kursa and E. Wagner, *Gene therapy*, 2001, **8**, 28-40.
7. H. Tian, Z. Guo, L. Lin, Z. Jiao, J. Chen, S. Gao, X. Zhu and X. Chen, *Journal of Controlled Release*, 2014, **174**, 117-125.
8. A. Kichler, M. Chillon, C. Leborgne, O. Danos and B. t. Frisch, *Journal of controlled release*, 2002, **81**, 379-388.
9. M. Jäger, S. Schubert, S. Ochrimenko, D. Fischer and U. S. Schubert, *Chemical Society Reviews*, 2012, **41**, 4755-4767.
10. M. Hornof, M. de la Fuente, M. Hallikainen, R. H. Tammi and A. Urtti, *The Journal of Gene Medicine*, 2008, **10**, 70-80.
11. T. Kurosaki, T. Kitahara, S. Kawakami, K. Nishida, J. Nakamura, M. Teshima, H. Nakagawa, Y. Kodama, H. To and H. Sasaki, *Biomaterials*, 2009, **30**, 4427-4434.
12. H. Tian, L. Lin, J. Chen, X. Chen, T. G. Park and A. Maruyama, *Journal of Controlled Release*, 2011, **155**, 47-53.
13. J. Sudimack and R. J. Lee, *Advanced Drug Delivery Reviews*, 2000, **41**, 147-162.
14. C. Peng, J. Qin, B. Zhou, Q. Chen, M. Shen, M. Zhu, X. Lu and X. Shi, *Polymer Chemistry*, 2013, **4**, 4412-4424.
15. T. Matini, N. Francini, A. Battocchio, S. G. Spain, G. Mantovani, M. J. Vicent, J. Sanchis, E. Gallon, F. Mastrotto and S. Salmaso, *Polymer Chemistry*, 2014, **5**, 1626-1636.
16. S. Y. Wong, J. M. Pelet and D. Putnam, *Progress in Polymer Science*, 2007, **32**, 799-837.
17. Z. Liu, Z. Zhang, C. Zhou and Y. Jiao, *Progress in Polymer Science*, 2010, **35**, 1144-1162.
18. M. Thomas and A. M. Klibanov, *Proceedings of the National Academy of Sciences*, 2002, **99**, 14640-14645.
19. A. Swami, A. Aggarwal, A. Pathak, S. Patnaik, P. Kumar, Y. Singh and K. Gupta, *International journal of pharmaceutics*, 2007, **335**, 180-192.
20. J. Yang, Y. Liu, H. Wang, L. Liu, W. Wang, C. Wang, Q. Wang and W. Liu, *Biomaterials*, 2012, **33**, 604-613.
21. X. Liu, J. Zhang and D. M. Lynn, *Soft Matter*, 2008, **4**, 1688-1695.
22. Z. Zhou, Y. Shen, J. Tang, M. Fan, E. A. Van Kirk, W. J. Murdoch and M. Radosz, *Advanced Functional Materials*, 2009, **19**, 3580-3589.
23. P. Xu, E. A. Van Kirk, Y. Zhan, W. J. Murdoch, M. Radosz and Y. Shen, *Angewandte Chemie International Edition*, 2007, **46**, 4999-5002.
24. Y. Lee, K. Miyata, M. Oba, T. Ishii, S. Fukushima, M. Han, H. Koyama, N. Nishiyama and K. Kataoka, *Angewandte Chemie*, 2008, **120**, 5241-5244.
25. M. Wang, H. Hu, Y. Sun, L. Qiu, J. Zhang, G. Guan, X. Zhao, M. Qiao, L. Cheng and L. Cheng, *Biomaterials*, 2013, **34**, 10120-10132.
26. L. Jia, Z. Li, D. Zhang, Q. Zhang, J. Shen, H. Guo, X. Tian, G. Liu, D. Zheng and L. Qi, *Polym. Chem.*, 2012, **4**, 156-165.
27. B. Wang, C. He, C. Tang and C. Yin, *Biomaterials*, 2011, **32**, 4630-4638.

28. A. Gautam, C. L. Densmore, E. Golunski, B. Xu and J. C. Waldrep, *Molecular Therapy*, 2001, **3**, 551-556.
29. N. D. Sonawane, F. C. Szoka and A. S. Verkman, *Journal of Biological Chemistry*, 2003, **278**, 44826-44831.
30. C. Arigita, N. J. Zuidam, D. J. Crommelin and W. E. Hennink, *Pharmaceutical research*, 1999, **16**, 1534-1541.
31. M. J Tiera, Q. Shi, F. M Winnik and J. C Fernandes, *Current gene therapy*, 2011, **11**, 288-306.
32. J. M. Saul, A. Annapragada, J. V. Natarajan and R. V. Bellamkonda, *Journal of Controlled Release*, 2003, **92**, 49-67.
33. H. S. Yoo and T. G. Park, *Journal of Controlled Release*, 2004, **100**, 247-256.
34. M. Neu, D. Fischer and T. Kissel, *The Journal of Gene Medicine*, 2005, **7**, 992-1009.
35. A. C. Hunter, *Advanced Drug Delivery Reviews*, 2006, **58**, 1523-1531.
36. Y. He, G. Cheng, L. Xie, Y. Nie, B. He and Z. Gu, *Biomaterials*, 2013, **34**, 1235-1245.
37. R. Kircheis, S. Schüller, S. Brunner, M. Ogris, K. H. Heider, W. Zauner and E. Wagner, *The Journal of Gene Medicine*, 1999, **1**, 111-120.
38. G.-J. Jeong, H.-M. Byun, J. M. Kim, H. Yoon, H.-G. Choi, W.-K. Kim, S.-J. Kim and Y.-K. Oh, *Journal of Controlled Release*, 2007, **118**, 118-125.

Table 1. Grafting level of LA, FA, HHPA, and the remaining free amino groups in LPHF.

Sample	Degree of grafted FA (%) [a]	Degree of grafted LA (%)[b]	Degree of grafted HHPA (%)[b]	Remaining free amino group (%)[b]
LPHF	2.02	4.57	42.85	50.56

[a] Determined from UV

[b] Calculated from ^{1}H NMR

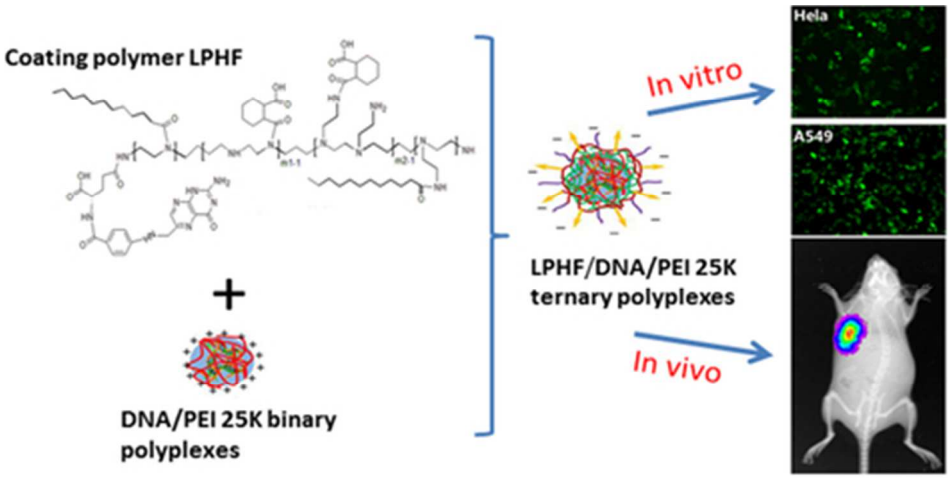

A novel coating polymer LPHF was developed for the first time to elevate the transfection efficiency of DP binary polyplexes in vitro and in vivo.
39x19mm (300 x 300 DPI)

Figure captions

Scheme 1. A schematic diagram showing polyplexes assembly, extracellular and intracellular trafficking of DPLPHF ternary polyplexes. DPLPHF ternary polyplexes accumulate at the tumor site via the EPR effect, followed by folate receptor-mediated and LA-facilitated synergetic cellular uptake. Coating polymer LPHF self-dissociates from the DP binary polyplexes in acidic endosomes and then DP binary polyplexes escape from endosomes through combined proton sponge effect of coating polymer LPHF and PEI 25K.

Fig. 1. Synthesis and confirmation of polymers. Synthesis scheme of LA-PEI (A), LA-PEI-FA (B), LA-PEI-HHPA-FA (C) and ^{1}H NMR of LA-PEI, LA-PEI-FA and LA-PEI-HHPA-FA (D).

Fig. 2. Acid-base titration profiles of PEI 1.8K, LPH, FPH, LPSF, LPHF and PEI 25K.

Fig. 3. (A) Particle size and zeta potential of DP binary polyplexes (w/w = 1) and DPLPHF ternary polyplexes (LPHF/PEI 25K = 1-80, w/w, charge ratio = 0.43-34.29) in HEPES buffer (20 mM, pH 7.4). Charge ratio between LPHF and DP binary polyplexes was presented in another x axis. Data were shown as mean ± S.D. (n = 3). (B) The competitive dissociation potential of DNA in DPLPHF ternary polyplexes (LPHF/PEI 25K = 1-80, w/w). (C) The protection effect of DPLPHF ternary polyplexes (LPHF/PEI 25K = 1-20, w/w) on DNA against the degradation of DNase in the serum. (D) Turbidity study of DP binary polyplexes (w/w = 1) and DPLPHF ternary polyplexes (LPHF/PEI 25K = 1-20, w/w) in BSA. Data were expressed as mean ± S.D. (n = 5). (E) Change in particle size of DP binary polyplexes (w/w = 1) and DPLPHF ternary polyplexes (LPHF/PEI 25K = 1-20, w/w) in BSA. Data were expressed as mean ± S.D. (n = 3). (F) TEM image of optimized DPLPHF polyplexes (LPHF/PEI 25K = 20, w/w). Scale bars: 200 nm.

Fig. 4. The pH-dependent charge-conversion and self-dissociation behaviour of optimized DPLPHF polyplexes. (A) Particle size and zeta potential of optimized DPLPHF polyplexes were measured under different pH conditions. Data were expressed as mean ± S.D. (n = 3). (B) The picture and calculated remaining LPHF polymers in the supernatant of different samples.

Fig. 5. Cell viability (% of control) of Hela and A549 cells. (A) Cells treated with gradient concentrations of PEI 25K or coating polymers. (B) Cells exposed to DP binary polyplexes or different ternary polyplexes containing gradient concentrations of PEI 25K/non-therapeutic pEGFP-C3. (C) Cells exposed to DP binary polyplexes or different ternary polyplexes containing therapeutic p53 at 2 μg/ml. Data were expressed as mean ± S.D. (n = 5). $^{*}P < 0.05$ and $^{**}P < 0.01$.

Fig. 6. Cellular uptake study of polyplexes. (A) Flow cytometric profiles of DP, DPLPH, DPFPH, DPLPSF and DPLPHF polyplexes with/without serum in Hela and A549 cells. (B) The fluorescence intensity of DP, DPLPH, DPFPH, DPLPSF and DPLPHF polyplexes with/without serum in Hela and A549 cells. (C) Flow cytometric profiles of DP, DPLPH, DPFPH, DPLPSF and DPLPHF polyplexes with/without serum in Hela cells pretreated with/without FA. (D) The fluorescence intensity of DP, DPLPH, DPFPH, DPLPSF and DPLPHF polyplexes with/without serum in Hela cells pretreated with/without FA. Data were expressed as mean ± S.D. (n = 5). $^{*}P < 0.05$ and $^{**}P < 0.01$.

Fig. 7. Transfection of pEGFP-C3 in Hela and A549 cells. (A) The fluorescence images of different polyplexes in two cell lines. (B) The flow cytometric analysis of GFP-expressing cells of different polyplexes in two cell lines. (C) Percentage of GFP-positive cells of different polyplexes in two cell lines. Data were expressed as mean ± S.D. (n = 5). $^{*}P < 0.05$ and $^{**}P < 0.01$.

Fig. 8. Intracellular trafficking of DP binary polyplexes (A) and DPLPHF ternary polyplexes (B) in Hela cells at different time intervals. The fluorescence signals were collected by CLSM with three channels: blue fluorescence from nuclei stained with Hoechst 33342, green fluorescence from FITC-labeled PEI 25K and red fluorescence from the Lyso-tracker stained endosomes. The final panels show the merged images of three channels.

Fig. 9. *In vivo* imaging of tumor targeting ability. (A) *In vivo* NIR fluorescence images after 12 h intravenous injection of Cy7-labled polyplexes in Hela tumor-bearing mice. *Ex vivo* NIR fluorescence images (B) and quantitative analysis (C) of representative tissues removed from tumor-bearing nude mice at 12 h post-injection. Quantitative analysis was expressed as photo flux per mm^2 of tumor. Results were expressed as mean ± S.D. ($n = 6$). $^{*}P < 0.05$ and $^{**}P < 0.01$.

Fig. 10. The tumor volume (A) and body weight (B) analysis of Hela tumor-bearing BALB/c nude mice after administration of saline, DP, DPLPH, DPFPH, DPLPSF and DPLPHF polyplexes, respectively. The injection of formulations was repeated every 2 days for two weeks, the measurement of tumor size and mice body weight was performed before the injection. Results were represented as mean ± S.D. ($n = 6$). $^{*}P < 0.05$ and $^{**}P < 0.01$.

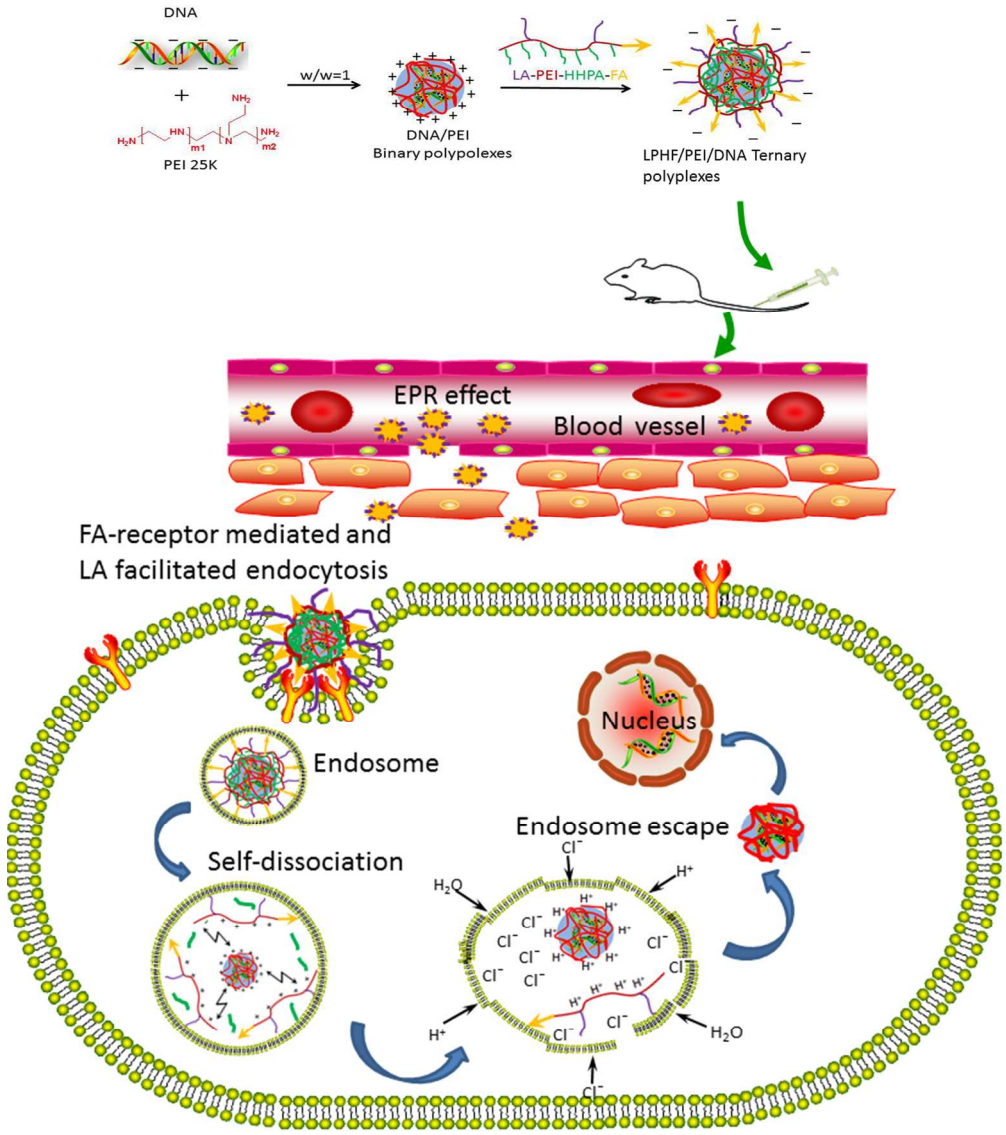

202x227mm (300 x 300 DPI)

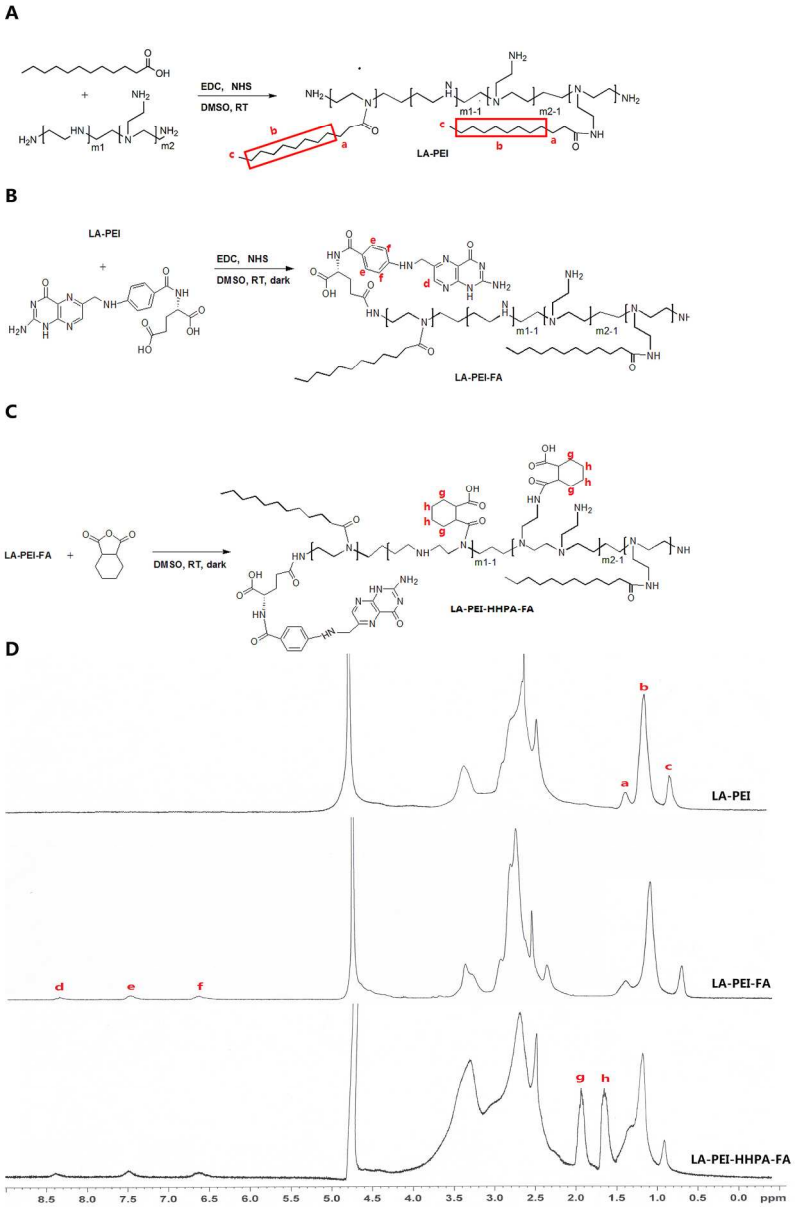

Fig. 1. Synthesis and confirmation of polymers. Synthesis scheme of LA-PEI (A), LA-PEI-FA (B), LA-PEI-HHPA-FA (C) and 1H NMR of LA-PEI, LA-PEI-FA and LA-PEI-HHPA-FA (D).
189x257mm (300 x 300 DPI)

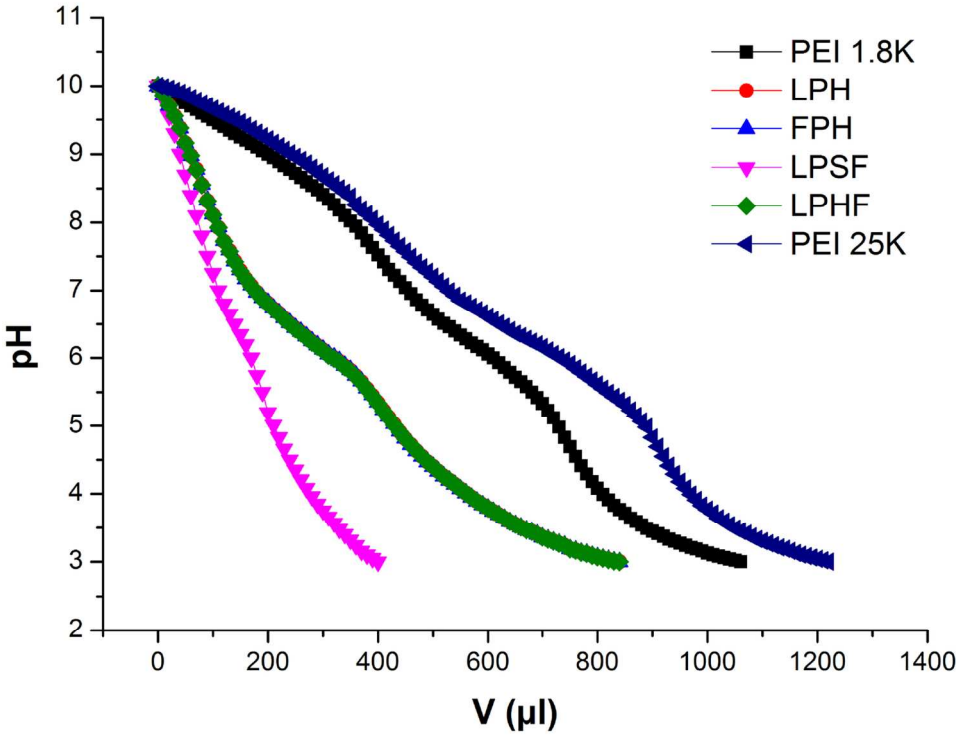

Acid-base titration profiles of PEI 1.8K, LPH, FPH, LPSF, LPHF and PEI 25K.
66x49mm (600 x 600 DPI)

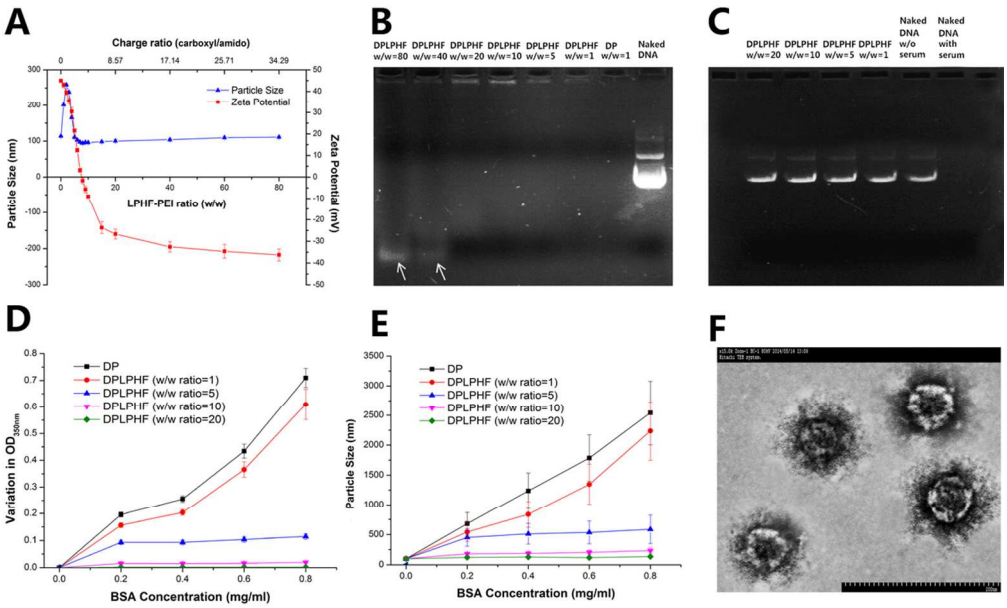

109x66mm (300 x 300 DPI)

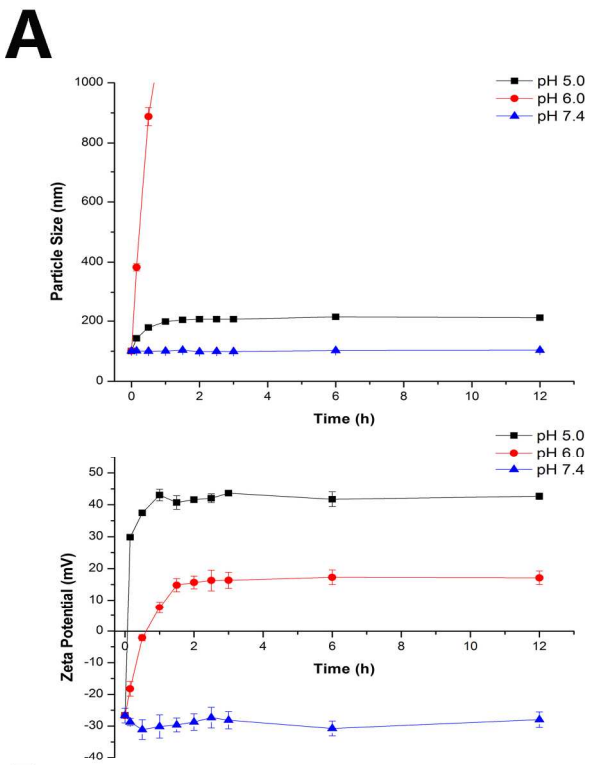

Sample	pH 7.4 (centrifuged)	pH 6.0 (centrifuged)	pH 5.0 (centrifuged)	pH 7.4 (untreated)
Remaining LPHF (%)	0	21.71	93.26	100

148x275mm (300 x 300 DPI)

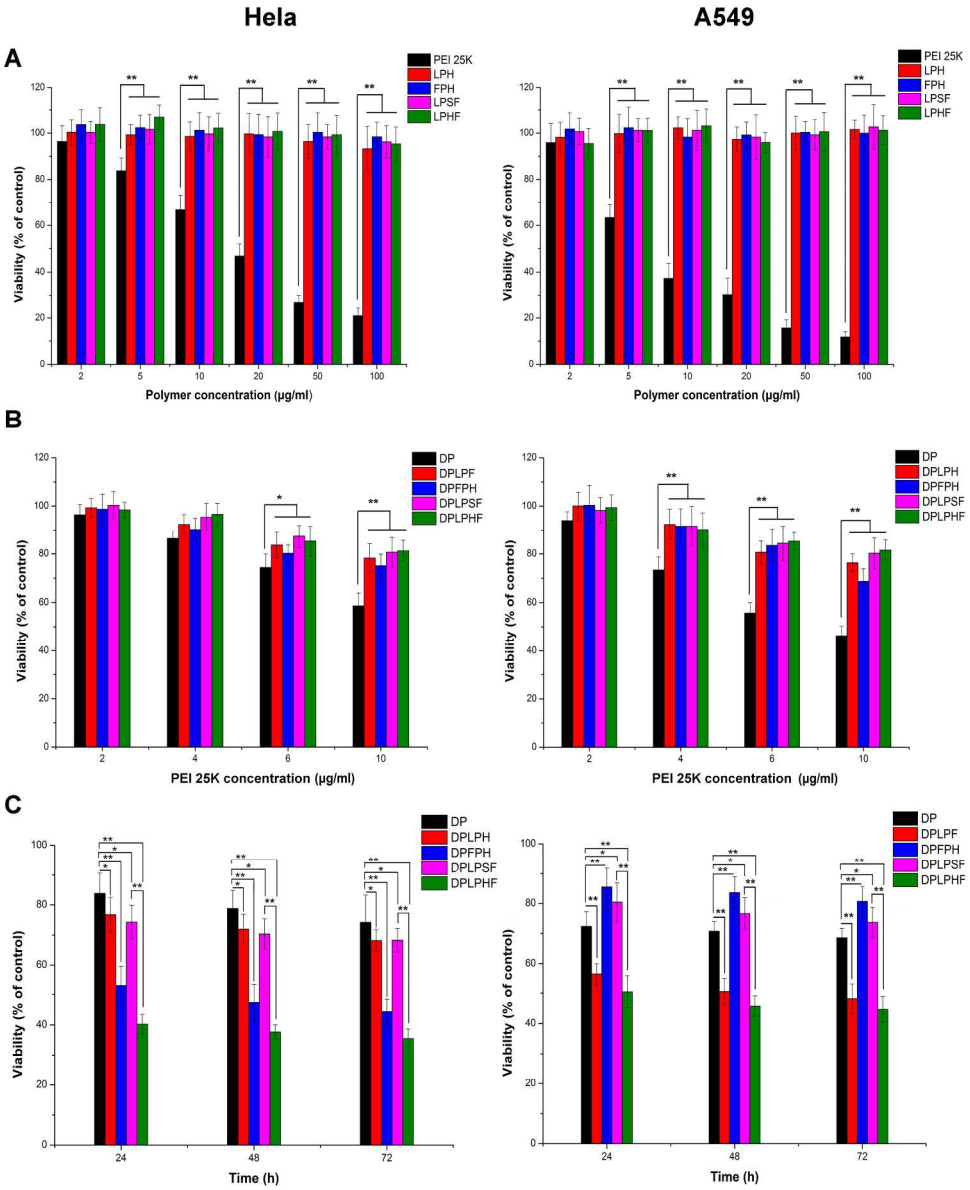

224x281mm (300 x 300 DPI)

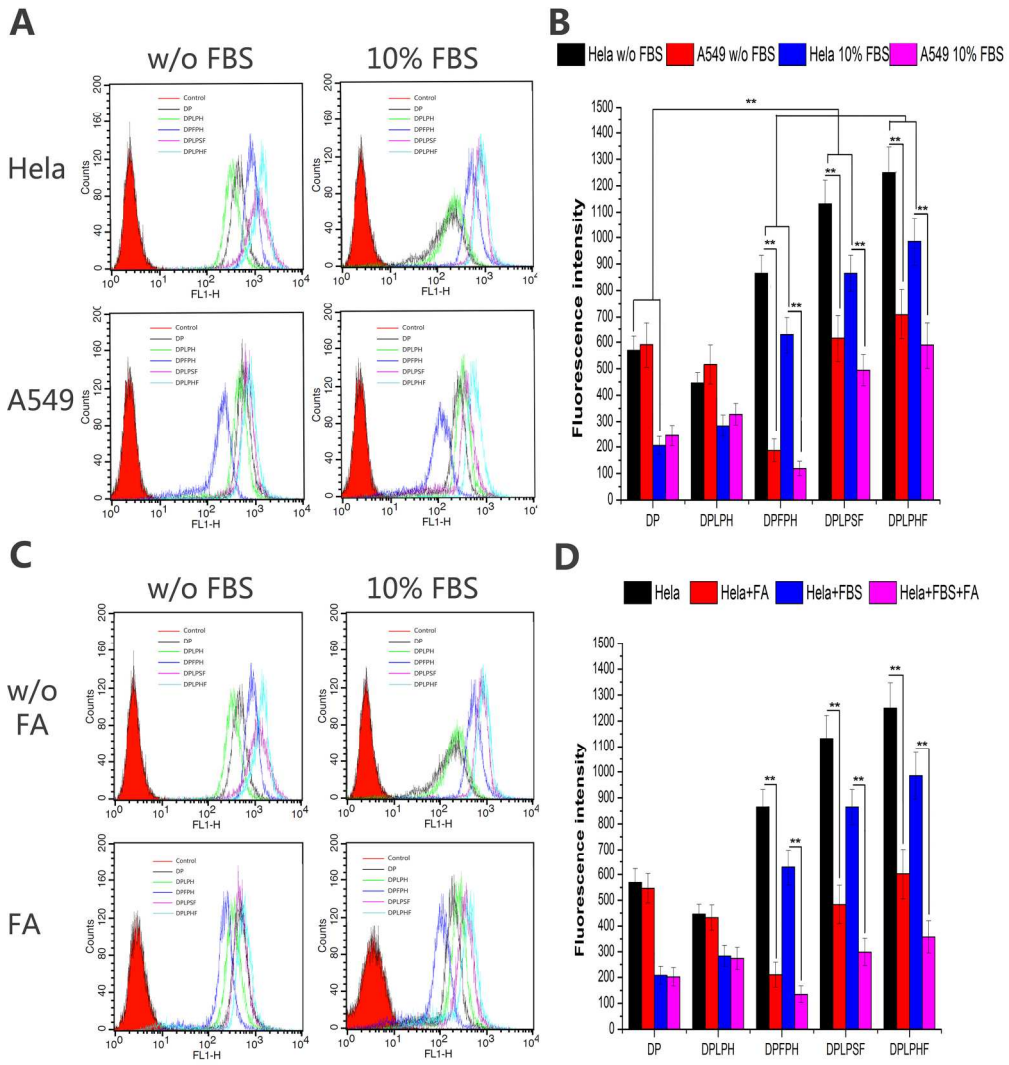

Cellular uptake study of polyplexes. (A) Flow cytometric profiles of DP, DPLPH, DPFPH, DPLPSF and DPLPHF polyplexes with/without serum in Hela and A549 cells. (B) The fluorescence intensity of DP, DPLPH, DPFPH, DPLPSF and DPLPHF polyplexes with/without serum in Hela and A549 cells. (C) Flow cytometric profiles of DP, DPLPH, DPFPH, DPLPSF and DPLPHF polyplexes with/without serum in Hela cells pretreated with/without FA. (D) The fluorescence intensity of DP, DPLPH, DPFPH, DPLPSF and DPLPHF polyplexes with/without serum in Hela cells pretreated with/without FA. Data were expressed as mean ± S.D. (n = 5). *P < 0.05 and **P < 0.01.
189x200mm (300 x 300 DPI)

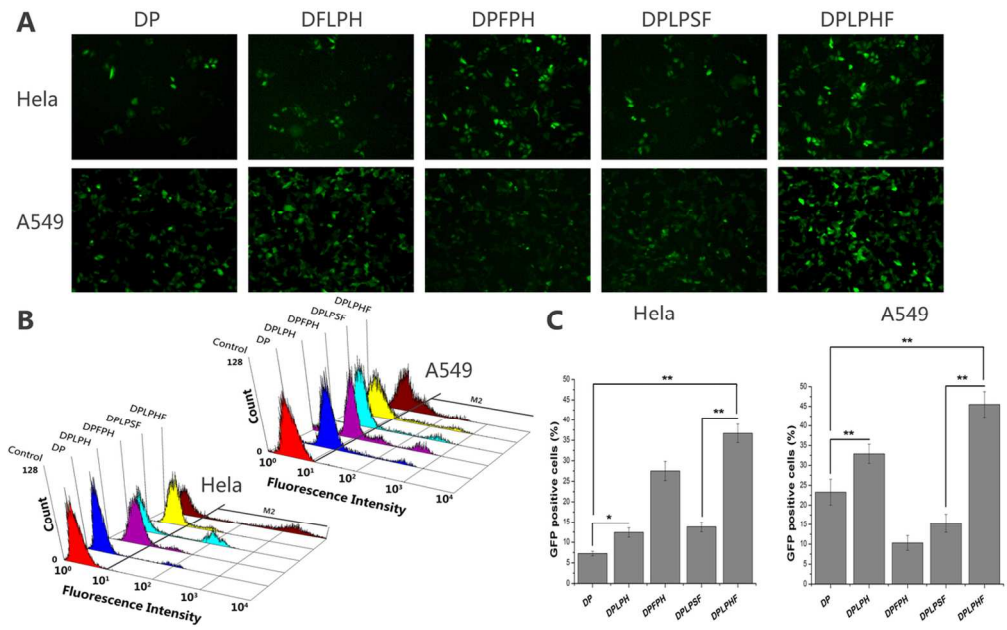

Transfection of pEGFP-C3 in Hela and A549 cells. (A) The fluorescence images of different polyplexes in two cell lines. (B) The flow cytometric analysis of GFP-expressing cells of different polyplexes in two cell lines. (C) Percentage of GFP-positive cells of different polyplexes in two cell lines. Data were expressed as mean ± S.D. (n = 5). *P < 0.05 and **P < 0.01.
112x69mm (300 x 300 DPI)

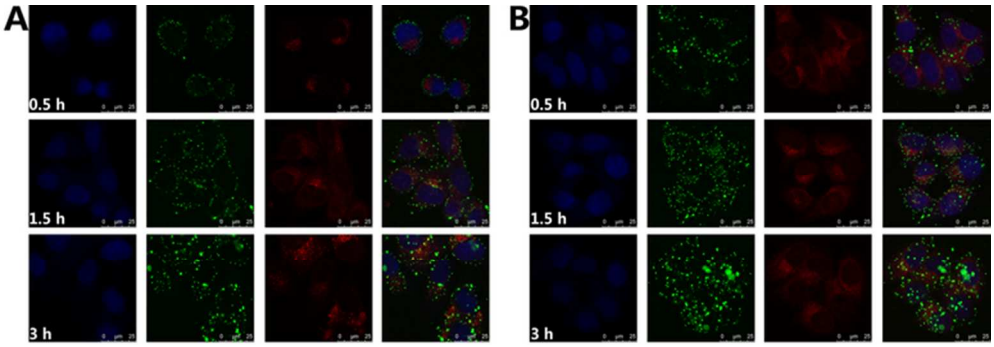

Intracellular trafficking of DP binary polyplexes (A) and DPLPHF ternary polyplexes (B) in Hela cells at different time intervals. The fluorescence signals were collected by CLSM with three channels: blue fluorescence from nuclei stained with Hoechst 33342, green fluorescence from FITC-labeled PEI 25K and red fluorescence from the Lyso-tracker stained endosomes. The final panels show the merged images of three channels.
66x22mm (300 x 300 DPI)

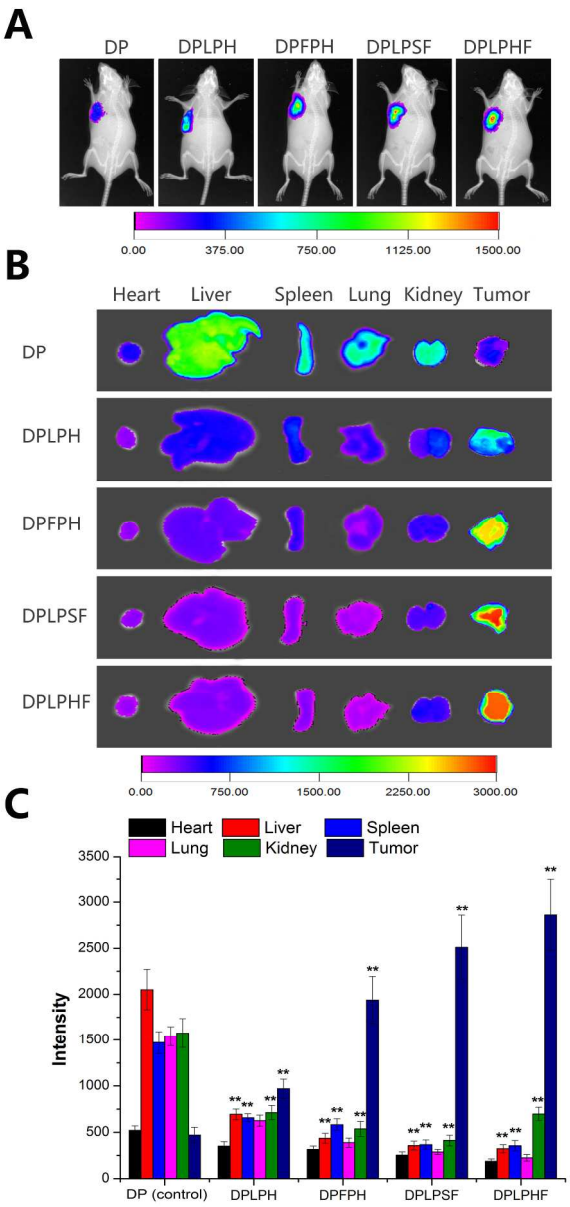

In vivo imaging of tumor targeting ability. (A) In vivo NIR fluorescence images after 12 h intravenous injection of Cy7-labled polyplexes in Hela tumor-bearing mice. Ex vivo NIR fluorescence images (B) and quantitative analysis (C) of representative tissues removed from tumor-bearing nude mice at 12 h post-injection. Quantitative analysis was expressed as photo flux per mm2 of tumor. Results were expressed as mean ± S.D. (n = 6). *P < 0.05 and **P < 0.01.
189x401mm (300 x 300 DPI)

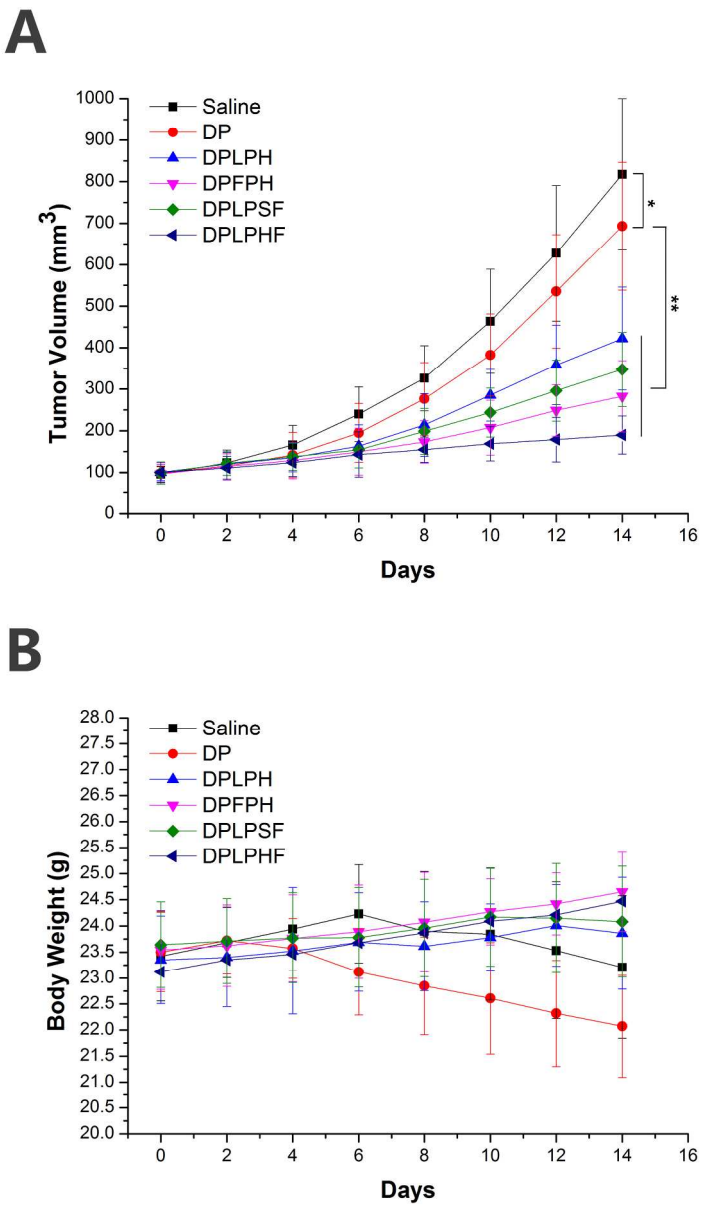

The tumor volume (A) and body weight (B) analysis of Hela tumor-bearing BALB/c nude mice after administration of saline, DP, DPLPH, DPFPH, DPLPSF and DPLPHF polyplexes, respectively. The injection of formulations was repeated every 2 days for two weeks, the measurement of tumor size and mice body weight was performed before the injection. Results were represented as mean ± S.D. (n = 6). *P < 0.05 and **P < 0.01.
131x192mm (600 x 600 DPI)